METHOD OF DETERMINING THE ULTIMATE DYNAMIC COMPRESSION PATTERNS FOR SOILS AND POROUS MEDIA RESPONSIVE TO THE STRAIN RATE

A. I. Kotov and G. V. Rykov

UDC 624.131+539.215

For media of the type of soils which are responsive to the strain rate, the question of determining the ultimate dynamic compression patterns corresponding to an instantaneous loading ($\dot{\varepsilon}=\infty$) [1, 2] is essential. Up to now such patterns have been determined on the front of a shock being propagated in a soil mass during the explosion of high-explosive charges [3-5] or during impact of a mass having a sufficiently high initial velocity on a soil specimen [6]. The method mentioned cannot be used during continuous compression-wave propagation in soils.

The relation between the uniaxial compression (tension) pattern and the propagation velocity for weak perturbations [7, 8] was used for elastic and elastoplastic media with nonlinear characteristics in order to determine dynamic tension patterns.

§1. The method under consideration is based on the relationship between the propagation velocities of weak perturbations in a compressed medium and the ultimate dynamic pattern $\varphi(\varepsilon)$ ($\dot{\varepsilon}=\infty$) in a viscoplastic medium. It is assumed that the fundamental properties of the soils and the porous media being considered under short-lived dynamic loads are described sufficiently accurately when subjected to uniaxial compression by a strain law of the type [9, 10]

$$\frac{\partial\varepsilon}{\partial t}=G(\sigma_1-f(\varepsilon))+\begin{cases}\dfrac{1}{E(\varepsilon)}\dfrac{\partial\sigma_1}{\partial t}, & \dfrac{\partial\sigma_1}{\partial t}\geqslant 0,\\ \dfrac{1}{E_*(\varepsilon)}\dfrac{\partial\sigma_1}{\partial t}, & \dfrac{\partial\sigma_1}{\partial t}<0,\end{cases} \tag{1.1}$$

where σ_1 is the greatest principal stress; $E(\varepsilon)$ is the variable strain modulus under loading ($\partial\sigma_1/\partial t\geq 0$); $E_*(\varepsilon)$ is the variable strain modulus under unloading ($\partial\sigma_1/\partial t<0$); $G>0$ for $\sigma_1>f(\varepsilon)$ and $G\equiv 0$ for $\sigma_1\leq f(\varepsilon)$; $f(\varepsilon)$ is the statistical compression pattern for $\dot{\varepsilon}=0$.

For $E_*(\varepsilon)=E(\varepsilon)$, the relation (1.1) agrees with the strain law examined in [11, 12]. An analogous model was examined in [13] in application to explosive wave propagation in soils. In particular, it follows from [9, 13] that the relationship between the propagation velocity of small perturbations $a(\varepsilon)$ and the ultimate dynamic pattern $\varphi(\varepsilon)$ ($\dot{\varepsilon}=\infty$) is determined by the relationship

$$E(\varepsilon)=d\varphi(\varepsilon)/d\varepsilon=\rho_0a^2(\varepsilon). \tag{1.2}$$

By integrating, we obtain the ultimate dynamic pattern from (1.2):

$$\varphi(\varepsilon)=\int_0^\varepsilon E(\xi)\,d\xi,\quad \dot{\varepsilon}=\infty. \tag{1.3}$$

For the strain law (1.1), the relationship (1.3) will correspond to the loading condition ($\partial\sigma_1/\partial t\geq 0$). For unloading ($\partial\sigma_1/\partial t<0$) and for $\sigma_1<f(\varepsilon)$ we analogously obtain

$$\varphi_*(\varepsilon,\varepsilon_*)=\sigma_{1_*}+\int_{\varepsilon_*}^{\varepsilon}E_*(\xi)\,d\xi,$$

where σ_{1*}, ε_* are the stress and strain achieved at the time when the condition $\sigma_1=f(\varepsilon)$ is satisfied.

Moscow. Translated from Zhurnal Prikladnoi Mekhaniki i Tekhnicheskoi Fiziki, No. 2, pp. 130-134, March-April, 1977. Original article submitted March 26, 1976.

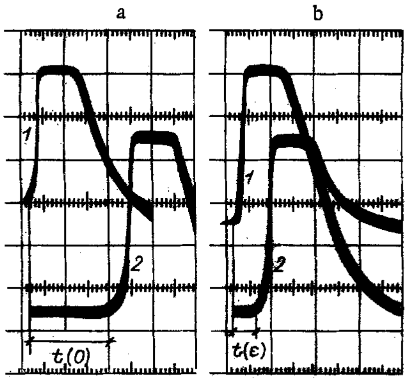

Fig. 1

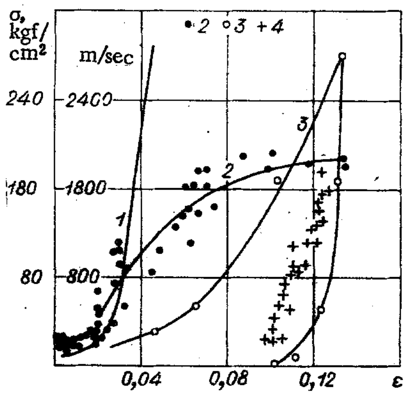

Fig. 2

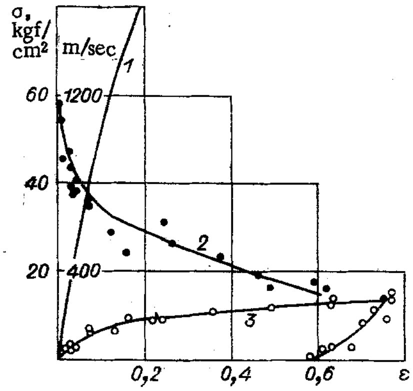

Fig. 3

Therefore, by knowing the dependence $a(\varepsilon)$ from experiment, the ultimate dynamic pattern $\varphi(\varepsilon)(\dot{\varepsilon} = \infty)$ under loading as well as the pattern $\varphi_*(\varepsilon, \varepsilon_*)$ for $\sigma_1 < f(\varepsilon)$ can be constructed.

However, one circumstance must be noted. It has been shown in [14] that for a strain law of the type (1.1), a situation is possible where weak discontinuities are not propagated at the velocity of the characteristics (the case of almost self-similar motion). At the same time, it follows from [14] that such a finite distance x_* can always be found when weak perturbations will be propagated at the velocity $a(\varepsilon)$ for $x < x_*$.

Therefore, for a sufficiently small specimen height h_0 the propagation velocity of weak perturbations will always equal the characteristic velocity. It hence also follows that such a method may turn out to be unsuitable for long rods from materials possessing viscous properties [8].

§2. To determine the dependence $a(\varepsilon)$ under laboratory conditions, a specimen of material is subjected to static loading by a load σ_{1i} which is varied in steps $(i = 1, 2, \ldots, n)$.

The static strain ε_i and the corresponding time $t_i = t(\varepsilon_i)$ for a wave of weak discontinuity to traverse a distance equal to the specimen height after a previous loading $h_i = h(\varepsilon_{i-1})$ are hence determined. For a sufficiently low specimen height the propagation velocity of a wave of weak discontinuity is defined as the mean

$$a(\varepsilon_i) = h_i/t_i,\ i = 1, 2, \ldots, n.$$

Results of investigating the ultimate dynamic compression patterns of sandy soil with the volume weight of the skeleton $\gamma_0 = 1.50$ g/cm³ and the humidity $w = 0.003$ and of foam plastic of the type PKhV with the volume weight $\gamma_0 = 0.07$ g/cm³ tested in an apparatus described earlier in [2] are presented.

To measure the traversal time $t(\varepsilon_i)$ some changes were introduced in the apparatus. In particular, piezotransducers on the basis of a TsTS-19 ceramic, whose signals were recorded on an S1-33 electronic oscillograph, were mounted in place of the piston and base (central) strain gauges. The piston sensor had been constructed in the form of a moving module which could be displaced under impact by generating a wave of weak discontinuity in the specimen. This weak perturbation was produced for each value of ε_i because of impact of a 100-g ball falling on the module with the sensor. The weight of the moving module with the sensor was also 100 g. The ball fell from a height of 1-2 cm.

Oscillograms of signals characterizing the perturbation in a sandy soil specimen, as recorded by the piston 1 and base 2 sensors, are represented in Fig. 1a, b. The scale division on the oscillograms is $75 \cdot 10^{-6}$ sec (Fig. 1a) and $30 \cdot 10^{-6}$ sec (Fig. 1b). The corresponding values of the traversal time and the velocity $a(\varepsilon)$ for $\sigma_{10} = 0$ (Fig. 1a) are $t(0) = 139 \cdot 10^{-6}$ sec, and $a(0) = 215$ m/sec, while for $\sigma_{1n} = 283$ kgf/cm² (Fig. 1b), $t(\varepsilon_n) = 16.5 \cdot 10^{-6}$ sec, $a(\varepsilon_n) = 1810$ m/sec. The nature of the perturbations recorded in the foam-plastic specimens is analogous.

Appropriate experimental results for sandy soil (Fig. 2) and foam plastic (Fig. 3) are represented in Figs. 2 and 3. Plotted along the horizontal is the strain ε and the stress σ_1 and velocity $a(\varepsilon)$ along the vertical. The points and curves 2 hence correspond to $a(\varepsilon)$ and 3 to the static compression pattern $f(\varepsilon)$ obtained at the strain rate $\dot{\varepsilon} = 2.5 \cdot 10^{-4}$ sec⁻¹ for sand and $\dot{\varepsilon} = 2.5 \cdot 10^{-3}$ sec⁻¹ for the foam plastic. Points 4 in Fig. 2 correspond to the velocities $a_*(\varepsilon)$ for $\sigma_1 < f(\varepsilon)$. The dependences $a(\varepsilon)$ and $f(\varepsilon)$ are approximated by the following formulas:

for sand

$$a(\varepsilon)/a(0) = 1 + m_0\varepsilon, \quad 0 \leqslant \varepsilon \leqslant \varepsilon_1; \tag{2.1}$$

$$a(\varepsilon)/a(\varepsilon_1) = [1 + m_1(\varepsilon - \varepsilon_1)^{\nu_1}]^{1/2}, \quad \varepsilon_1 < \varepsilon \leqslant 0.12;$$

$$f(\varepsilon) = K(\varepsilon + m_2\varepsilon^{\nu_2}), \quad 0 \leqslant \varepsilon \leqslant 0.13; \tag{2.2}$$

for foam plastic

$$a(\varepsilon)/a(0) = 1 - m_1\varepsilon^{\nu_1}, \quad 0 \leqslant \varepsilon \leqslant 0.50; \tag{2.3}$$

$$f(\varepsilon) = \begin{cases} K\varepsilon, & 0 \leqslant \varepsilon \leqslant \varepsilon_s; \\ \sigma_s[1 + m_2(\varepsilon - \varepsilon_s)^{\nu_2}], & \varepsilon_s < \varepsilon \leqslant 0.70. \end{cases} \tag{2.4}$$

where $a(0) = 200$ m/sec; $m_0 = 37$; $a(\varepsilon_1) = 350$ m/sec; $\varepsilon_1 = 0.02$; $m_1 = 364$; $\nu_1 = 1.0$; $K = 550$ kgf/cm^2; $m_2 = 155$; $\nu_2 = 3.0$ in (2.1) and (2.2), while $a(0) = 1125$ m/sec; $m_1 = 0.89$; $\nu_1 = 0.36$; $\varepsilon_S = 0.0346$; $\sigma_S = 4.5$ kgf/cm^2; $K = 130$ kgf/cm^2; $m_2 = 2.30$; $\nu_2 = 0.46$ in (2.3) and (2.4).

The ultimate dynamic patterns (curves 1 in Figs. 2 and 3) are obtained from (2.1) and (2.3) in the following form by taking account of (1.3):

for sand

$$\varphi(\varepsilon) = \begin{cases} \frac{E_0}{3m_0}[(1 + m_0\varepsilon)^3 - 1], & 0 \leqslant \varepsilon \leqslant \varepsilon_1, \\ \sigma_0 + E_1[\varepsilon - \varepsilon_1 + m(\varepsilon - \varepsilon_1)^{\nu}], & \varepsilon_1 < \varepsilon \leqslant 0.12, \end{cases}$$

where $E_0 = 608$ kgf/cm^2; $m = 182$; $\nu = 2.0$; $E_1 = 1880$ kgf/cm^2; $\sigma_0 = 23.2$ kgf/cm^2 and

for foam plastic

$$\varphi(\varepsilon) = E_0\left(\varepsilon - \frac{2m_1}{1 + \nu_1}\varepsilon^{1+\nu_1} + \frac{m_1^2}{1 + 2\nu_1}\varepsilon^{1+2\nu_1}\right),$$

where $E_0 = 1000$ kgf/cm^2.

It is interesting to note the qualitative distinction in the nature of the pattern $\varphi(\varepsilon)(\dot{\varepsilon} = \infty)$ for sandy soil and for foam plastic. In the first case, the velocities $a(\varepsilon)$ grow with the increase in ε, while the condition $d^2\varphi/d\varepsilon^2 > 0$ holds for $\varphi(\varepsilon)$. For foam plastic $a(\varepsilon)$ decreases with the increase in ε and $d^2\varphi/d\varepsilon^2 < 0$ correspondingly (within the limits of the measured values of the stress).

The difference in the values of the propagation velocities of weak perturbations $a_*(\varepsilon)$ during unloading from $a(\varepsilon)$ during loading for the very same values of the strain ε (points 4 in Fig. 2) indicates that $E_*(\varepsilon) \neq E(\varepsilon)$ in a strain law of the type (1.1).

The results obtained confirm the data elucidated earlier in [2] about the substantial influence of the strain rate on the compressibility of sandy soils under short-lived loads.

Still more significant does the influence of the strain rate turn out to be on the compressibility of foam plastic for which the difference in the strains for $\dot{\varepsilon} = \infty$ and $\dot{\varepsilon} = 2.5 \cdot 10^{-3}$ sec^{-1} reaches 10-15-fold (for $\sigma_1 = 10$-12 kgf/cm^2).

LITERATURE CITED

1. V. V. Mel'nikov and G. V. Rykov, "On the influence of the strain rate on the compressibity of loess soils," Zh. Prikl. Mekh. Tekh. Fiz., No. 2, 158-160 (1965).
2. G. V. Rykov, "Influence of the strain rate on the compressibility and shear of sandy and clay soils under short-lived dynamic loads," Zh. Prikl. Mekh. Tekh. Fiz., No. 3, 155-160 (1969).
3. V. D. Alekseenko, S. S. Grigoryan, L. I. Koshelev, A. F. Novgorodov, and G. V. Rykov, "Stress wave measurement in soft soils," Zh. Prikl. Mekh. Tekh. Fiz., No. 2, 135-141 (1963).
4. G. V. Rykov, "Experimental investigation of the stress field during an explosion in sandy soil," Zh. Prikl. Mekh. Tekh. Fiz., No. 1, 85-89 (1964).
5. G. M. Lyakhov, Principles of Explosion on Dynamics in Soils and Liquid Media [in Russian], Nedra, Moscow (1964), pp. 61-66.
6. V. A. Lagunov and V. A. Stepanov, "Measurement of the dynamic compressibility of sand at high pressures," Zh. Prikl. Mekh. Tekh. Fiz., No. 1, 88-96 (1963).

7. G. I. Barenblatt, "On perturbation propagation in a medium with a nonlinear stress–strain dependence," Prikl. Mat. Mekh., 17, No. 4 (1953).
8. A. A. Il'yushin and V. S. Lenskii, Strength of Materials [in Russian], Fizmatgiz, Moscow (1959), p. 277.
9. J. A. Lubliner, "A general theory of strain-rate dependent plastic wave propagation in bars," J. Mech. Phys. Solids, 12, 59-65 (1964).
10. N. Christescu, "On longitudinal wave propagation in thin elastoviscoplastic rods," in: Mekhanika [Periodic Collection of Translations of Foreign Articles], No. 3 (1966), pp. 119-133.
11. V. V. Sokolovskii, "Propagation of elastoviscoplastic waves in rods," Prikl. Mat. Mekh., No. 3, 261-280 (1948).
12. L. Malvern, "Longitudinal wave propagation taking account of the influence of the strain rate," in: Mekhanika [Periodic Collection of Translations of Foreign Articles], No. 1 (1952), pp. 153-161.
13. A. N. Zubkova and G. V. Rykov, "One-dimensional stress wave propagation in a viscoplastic medium," in: Materials of the Fifth All-Union Symposium, October 4-7, 1971 [in Russian], Nauka, Alma-Ata (1973), pp. 165-173.
14. A. M. Skobeev, "Loading wave in a viscoplastic medium," Izv. Akad. Nauk SSSR, Mekh. Tverd. Tela, No. 2, 139-142 (1967).

SHIELD PROPERTIES OF A THIN PLATE UNDER HIGH-VELOCITY IMPACT

L. A. Merzhievskii and V. M. Titov

UDC 628.198.624

In perforating a thin plate (shield) a high-velocity particle (meteoroid) is shattered as the result of the wave processes which are generated within it. During the course of its deformation a velocity field arises in the particle; this field has a nonzero component perpendicular to the impact direction, so that the trajectories of the debris particles are at various angles to the trajectory of the particle; these debris particles then impact a target plate, placed behind the shield, over a much larger area than the cross-sectional area of the particle. This, together with the loss in momentum of the particle as it perforates the shield, determines the protective effect of the shield.

The process involved in the deformation and shattering of the particle in its collision with the shield was considered in [1]. In this paper we justify, based on the experiments conducted in [1], a method of quantitatively estimating the damage inflicted on the obstacle (target) protected by the shield. The method employed for accelerating steel spheres was described in [2]. In all our experiments we permitted a pressure of up to 1 mm Hg in the space between the shield and the target.

It is difficult to give a general description of the problem involving perforation of a shielded target, since the mechanism involved in explaining the target damage changes when the distance S between the target and the shield is varied. When S is small the impact onto the target is due to a nondiffuse (compact) debris cloud from a still deforming particle; as S increases, however, the damage to the target results in increasing measure, from the impact of the coarsest particles present in the concentrated debris field. It is necessary, therefore, to estimate the applicable interval over which the quantity $S_1 = S/d_0$ (where d_0 is the diameter of the impacting particle) varies corresponding to a given one of these target damage mechanisms. When the target chosen is thick (semiinfinite), we can use, as a quantitative measure of target damage and, hence also, of shield effectiveness, the depth h of the largest of the craters formed in the target.

The experimental results obtained are shown in Fig. 1 in terms of a set of curves showing $h_1 = h/d_0$ plotted against S_1; curve 1 corresponds to an impact of aluminum on aluminum with $\delta/d_0 = 0.3$ (δ is the shield thickness); curves 2, 3, and 4, with $\delta/d_0 = 0.2$, 0.6, and 0.67, respectively, correspond to impacts of steel onto D16. Here and henceforth, the first-named material corresponds to that of the particle and the second-named

Novosibirsk. Translated from Zhurnal Prikladnoi Mekhaniki i Tekhnicheskoi Fiziki, No. 2, pp. 134-139, March-April, 1977. Original article submitted March 19, 1976.